General Disclaimer

One or more of the Following Statements may affect this Document

- This document has been reproduced from the best copy furnished by the organizational source. It is being released in the interest of making available as much information as possible.

- This document may contain data, which exceeds the sheet parameters. It was furnished in this condition by the organizational source and is the best copy available.

- This document may contain tone-on-tone or color graphs, charts and/or pictures, which have been reproduced in black and white.

- This document is paginated as submitted by the original source.

- Portions of this document are not fully legible due to the historical nature of some of the material. However, it is the best reproduction available from the original submission.

NASA TECHNICAL MEMORANDUM

NASA TM-73867

NASA TM-73867

(NASA-TM-73867) INTERACTION OF LARGE, HIGH POWER SYSTEMS WITH OPERATIONAL ORBIT CHARGED PARTICLE ENVIRONMENTS (NASA) 19 p HC A02/MF A01 CSCL 22A

N78-16076

Unclas
G3/12 02581

INTERACTION OF LARGE, HIGH POWER SYSTEMS WITH OPERATIONAL ORBIT CHARGED PARTICLE ENVIRONMENTS

by Carolyn K. Purvis, N. John Stevens, and Frank D. Berkopec
Lewis Research Center
Cleveland, Ohio 44135

TECHNICAL PAPER presented at the
Meeting on Long Range Planning for the
Industrial Phase of Space Exploration
sponsored by the American Astronautical Society
San Francisco, California, October 18-20, 1977

INTERACTION OF LARGE, HIGH POWER SYSTEMS WITH OPERATIONAL ORBIT CHARGED PARTICLE ENVIRONMENTS

by *Carolyn K. Purvis, †N. John Stevens,
and ‡Frank D. Berkopec

Concepts are presently being advanced for space systems to be used for such activities as manufacturing, Earth observations, scientific exploration, power generation and human habitation, in locations ranging from low Earth orbit (300 - 500 km) to geosynchronous orbit and beyond. Many of these systems concepts envision large structures and high power levels, and consequently higher operating voltages than have been used in space to date. The potential impact of interactions of space systems with their operational orbit charged particle environments on the systems' performance must be accounted for in the design process. A potentially hazardous spacecraft-environment interaction is discussed in this paper. This is the interaction of large high voltage systems with low energy (<50 eV) plasmas which can result in loss of power and/or arcing. The impact of this class of interactions on system operation is most severe at low orbits where the ambient plasmas are densest. Results of experimental work and predictions of simple analytical models are presented and their implications for design of space systems are discussed.

E-9459

INTRODUCTION

Studies are presently being conducted for space systems to be used for such diverse activities as manufacturing, scientific exploration, power generation and human habitation in locations ranging from low Earth orbit (300 - 400 km) to geosynchronous orbit and beyond[1, 2, 3, 4]. Many concepts for such systems envision large complex structures and high power levels. Consequently, for higher electrical efficiency, higher operating voltages than those used to date are being proposed. In designing these new systems, care must be taken

* Aerospace Engineer, NASA-Lewis Research Center, Cleveland, Ohio 44135.
† Head, Spacecraft Environment Section, NASA-Lewis Research Center, Cleveland, Ohio 44135.
‡ Aerospace Engineer, NASA-Lewis Research Center, Cleveland, Ohio 44135.

STAR Category 18

to consider the influence of interactions with orbital charged particle environments on a system's operation. These systems will be expensive to build and launch; their economic feasibility is strongly dependent on optimal design and long term reliability. This report presents a preliminary evaluation of the effects of charged particle interactions with space systems in Earth orbits ranging from shuttle altitudes to geosynchronous altitude (fig. 1).

The interactions of space systems with their charged particle environments can be divided into three general types, with each comprising an interaction of the space system with particles of a characteristic energy level.

The first of these types is the interaction of high voltage systems with the thermal plasmas (temperature <2 eV) of the plasmasphere. These plasmas range in density, composition and temperature as a function of altitude. Typical random electron current and ram ion current (resulting from spacecraft motion) as functions of altitude are shown in figure 2[5]. This type of interaction is due to the voltage differences among various portions of the space system. Spacecraft flown to date have had low voltage power systems. Therefore the impact on their performance has been negligible. However, for the new generation of high power high voltage systems now being proposed, these interactions must be considered.

The primary emphasis of this paper is on the high voltage system interactions. The concept of the basic mechanism involved is discussed, preliminary results of experiments with a solar array segment are presented, and a simple model of a large solar array in low Earth orbit and in geosynchronous orbit is used in a preliminary evaluation of the impact of these interactions on the performance of a space system.

The second general type of interaction is the charging of spacecraft in geosynchronous orbit by kilowatt particles (~1 to ~50 keV)(see fig. 2). During geomagnetic substorm activity, clouds of kilovolt electrons and protons are injected into the midnight sector of the magnetosphere, and are observed at geosynchronous orbit[6]. These particles are known to charge spacecraft negatively with respect to plasma potential to kilovolt levels in eclipse, and to hundreds of volts in sunlight[7]. Spacecraft charging and its impact on space systems is the subject of an ongoing investigation[8]. There is a substantial literature on spacecraft charging[9, 10, 11] and it will not be discussed further here.

The final category of interactions is the radiation damage to spacecraft components caused by high energy particles (~100 keV and greater). This type of interaction is a known phenomenon and will not be discussed further.

HIGH VOLTAGE SYSTEM/THERMAL ENVIRONMENT INTERACTIONS

Basic Interaction Mechanism Concept

It is well known from probe theory[12] that any surface placed in a plasma will collect current from the plasma and that this collection is dependent upon the surface voltage. Any system immersed in a plasma will come into equilibrium with the plasma by acquiring the charges necessary to make the net current between the system and the plasma zero.

In general, the electron flux (and therefore electron current density) in a plasma is larger than the ion flux. A conducting surface (simple probe) placed in a plasma will thus collect more electrons than ions. This will cause it to take on a negative voltage with respect to the plasma. It will then collect fewer electrons and more ions. In equilibrium it will have acquired negative potential such that the electron and ion currents to it are equal, i.e. it is collecting net zero current. Typically this negative "floating" potential will be of order the electron energy.

In the case of a system with a distributed voltage, a solar array for example, the system will float at voltages relative to the plasma so that the positive area collects electrons and the negative area collects an equal current of ions. Figure 3 depicts this concept for a solar array having an operating voltage V_{op} with a linear distribution along the panel length. The negative portion of the array collects ions, and the positive portion electrons. Since, in general, electron fluxes are higher than ion fluxes in a plasma, a larger area is required for collecting ions. Consequently, in equilibrium, the magnitude of the negative voltage (collecting ions) will be larger than that of the positive voltage.

The net effect of the process of particle collection is that a current (I_{PLASMA}) passes through the plasma effectively creating a parasitic load (R_{PLASMA}) in parallel with the electrical load of the array. This results in a loss of useable array power.

To calculate the magnitude of this effect, it is necessary to make an estimate of the current collection of an array which has small biased conductor areas surrounded by large areas of insulation. This estimate is made with the help of data from an experiment using a biased array segment. The blowup in figure 3 shows the construction of a current lightweight large solar array design. The sketch is a cross section through a single cell. The cells are 2 x 4 cm and 0.02 cm (8 mils) thick with wraparound contacts exposed only on the edges, and are covered by 0.015 cm (6 mil) fused silica cover glasses. They are mounted on a substrate consisting of copper interconnects sandwiched between two layers of 0.001 cm (0.5 mil) kapton. The cell connectors are welded to the interconnects through holes in the kapton; there are access holes to the copper interconnects in the back (non cell) side of the array. Thus, while each surface of the array is largely covered with insulators, there is some exposed metal on each side.

A segment of an array of this construction has been tested in the Lewis Research Center's (LeRC) geomagnetic substorm simulation facility[13]. The segment, obtained from the Marshall Space Flight Center, is 14 cm x 20 cm (see fig. 4) and has 20 cells mounted in a series-parallel circuit. A plasma was generated by ionizing nitrogen gas in the facility's plasma source. The properties of the environment for the tests conducted on this segment were: ambient pressure $\sim 10^{-6}$ torr, plasma density $\sim 10^{+5}/cm^3$ and electron temperature ~3 eV. The electrical circuit of the array was biased to ±1 KV in a series of steps by means of a power supply outside the tank. The voltage profiles across the array segment were obtained by sweeping the facility electrostatic probe across the sample at fixed time interval. Thus, transient to steady-state profiles were obtained. The tests were conducted twice, once with the probe surveying the cell side and secondly with the substrate being surveyed. All test results presented here were obtained without sunlight and with the sample nominally at room temperature. Prior testing has verified that sunlight and temperature do not cause significant changes in the test results.

Voltage profiles obtained with this sample are shown in figure 5 for selected values of applied voltage. The voltage probe sweeps across the sample about 3 mm from the cover slide surface.

When the segment is biased positively, the exposed interconnects collect electrons from the environment. When the applied bias voltage is less than +190

volts, the surface voltage profile shows that the bias voltage appears only at the interconnect regions with the cover slide surfaces remaining essentially at zero voltage. For this applied voltage regime, the electron coupling current collected is proportional to the applied voltage and the area of the interconnects.

When the applied voltage is greater than 190 volts, there is a transition in the collection phenomenon. There is a "snap-over" or sudden change in the surface voltage profiles. When this snap-over occurs, the bias voltage is no longer constrained to the interconnect region, but expands to encompass the cover slides as well. This results in essentially a flat surface voltage across the array segment. The magnitude of this measured surface voltage is about 50 volts less than the applied potential. The electron coupling current collected in this voltage regime is proportional to the applied voltage (less than 50 volts) and the array area. It is believed that this snap-over condition occurs due to secondary emission from the cover slides. The details of the theory to explain this phenomenon are being developed.

When the array segment is biased negatively, a different phenomenon occurs. The voltage profiles indicate that ion collection is limited to the exposed conductor areas and that ion attractive potentials are significantly less than applied potentials. There is an additional phenomenon that occurs when the segment is biased negatively to a value greater than 700 volts: the segment arcs (see fig. 4). This occurs on both the front and rear sides of the array (at times simultaneous front and back discharges were observed). This arcing occurred continuously during the testing of the segment at a rate of about 3 per minute. Testing at different plasma densities indicates that arcing occurs at different values of applied voltage, being higher at lower densities. At simulated geosynchronous altitude conditions this breakdown is expected at ~-8 to -10 KV based on previous LeRC experiments.

Experimental results presented here are preliminary. Trends observed have been obtained with different samples in this and other facilities[14, 15]. Hence, it is believed that the array will collect electron currents as a function of exposed collector area and applied voltage up to positive values of 150 to 190 volts. Above this threshold, the current collection will be proportional to the panel area. At negative applied voltages, the ion current will be dependent only on the exposed conductor area. The detailed investigation of this phenomenon (both analytical and experimental) is continuing.

Simple Model for Space System

Calculations of array voltages and parasitic current collected as functions of array operating voltage were made for environments expected at 400 km and geosynchronous (both equatorial), using a simple model. The "space system" considered is that of figure 3, a 20 meter x 250 meter solar array with a power output of 500 kw (~100 W/m^2). Some of the assumptions incorporated in the model are illustrated in figure 6. Two voltages for current collection are assumed, V_+ and V_-. These are treated throughout this paper as magnitudes i.e. positive quantities. As figure 6(a) illustrates, $V_+ + V_- = 1/2\ V_{op}$. Because the voltage gradient is assumed constant along the array, the length of the array available to collect ions or electrons is proportional to the ion or electron collecting voltage, i.e. $\ell_+/\ell_- = V_+/V_-$. V_+ and V_- are expected to be different because the electron and ion fluxes are different, as has been noted.

The condition for the array to be in equilibrium with the surrounding plasma is that the net current to the array be zero, or, equivalently, that the magnitude of the electron current collected equal that of the ion current:

$$j_e A_+ = j_i A_- \tag{1}$$

Here, j_e and j_i are the magnitudes of the electron and ion current densities striking the array, and A_+ or A_- is the positive or negative array area collecting electrons or ions.

The electron current density j_e is taken to be the random electron current density. It is assumed that secondary electrons due to electron impact on the positive section of the array will be reattracted and thus contributed no net current density.

The ion current density j_i is taken to be the sum of two terms, one due to incoming ions, and the other to secondary electrons from ion impact. The latter term is included because such secondary electrons will be repelled from the negative side of the array and therefore add to the effective "ion" current. For purposes of this model, the current density due to these secondary electrons is taken to be

$$j_{is} = j_{io}\left(1 + \frac{1.36\sqrt{V_-}}{1 + 40/V_-}\right)$$

(V_- in kV) (2)

which gives a good fit to experimental data for protons normally incident on aluminum[16]. Here, j_{io} is the current density of incident ions and V_- is the negative array voltage, which corresponds to the energy of the ions on impact. While it is recognized that equation (2) is for protons rather than heavier ions (eg 0^+), it should give some estimate (within a factor 2 in the yield) of the effect of the secondary electrons on the current balance.

Another consideration in the ion current density is the ram effect which occurs in low Earth orbit, where the velocity of the space vehicle through the plasma is greater than the thermal velocity of the ions. The situation for an orbiting solar array is sketched in figure 6(c). Assuming the array is oriented for normal incidence to sunlight, the velocity vector rotates around the array once per orbit. When $\vec{v}$ is normal to the plane of the array there is a ram ion current on either the cell side or the back of the array. In this case $j_{io} = j_{iram}$, and ion collection takes place only on one side of the array. It is thus assumed that the ion density in the wake is sufficiently low that the contribution to the ion current from ions in the wake is negligible. When $\vec{v}$ is parallel to the array plane, only one edge sees the ram ions. As a limiting case of this condition, (assuming zero frontal area), j_{io} is taken to be just the thermal ion current for this orientation, and ion collection occurs on both sides of the array. That is, the collection is assumed to be from an isotropic plasma in this orientation. For either case, $j_i = j_{io} + j_{is}$.

There is no ram effect for electron collection, because the electron thermal velocities are much greater than the space system's orbital velocity. Thus, electron collection is always assumed to be from an isotropic plasma i. e. electron collection occurs on both sides of the array.

The areas for collection of electrons (A_+) and ions (A_-) are taken to be

$$A_+ = N_+ \ell_+ w_{eff+}$$
$$A_- = N_- \ell_- w_{eff-} \qquad (3)$$

where the + or - subscript refers to the positive or negative voltage portions which collect electrons or ions. A is the area for particle collection, ℓ is the length of the panel for collection, w_{eff} is the effective width for collection and N is the number of sides of the panel collecting (N = 1 or 2). The effective width w_{eff} is calculated from[17]

$$w_{eff\pm} = w + \pi r_{s\pm} \qquad (4)$$

where w is the panel width (20 meters) and $r_{s\pm}$ is the sheath radius (see fig. 6(b)) which is calculated from the Child-Langmiur relation

$$r_{s+}^2 = \frac{4\epsilon_o}{9}\sqrt{\frac{2e}{m_e}}\frac{V_{eff+}^{3/2}}{j_e} \qquad \text{(electrons)} \tag{5a}$$

$$r_{s-}^2 = \frac{4\epsilon_o}{9}\sqrt{\frac{2e}{m_i}}\frac{V_{eff-}^{3/2}}{j_i} \qquad \text{(ions)} \tag{5b}$$

and here, m_e or m_i is the mass of the electron or ion, e the electronic charge (singly charged ions are assumed), ϵ_o is the permittivity of free space (8.85 x 10^{-12} Farad/meter), and $V_{eff\pm}$ the effective potential.

$$V_{eff\pm} = fV_{\pm} \qquad \text{(Ref. 17)} \tag{6}$$

where f is the fraction of the panel area occupied by exposed metal. In the present calculation equation (6) was used to define V_{eff-} for all V_- since the experimental data indicate that the insulating surface in fact "shields" the voltage of the underlying cells for negative bias. Note that the data are for voltages $|V_-| \leq 1$ kV. It is entirely possible that a voltage snapover could occur for larger negative voltages, or in the presence of lower energy ions. For collection of electrons, equation (6) was used to define V_{eff+} for voltages $V_+ < 200$ volts. For $V_+ \geq 200$ volts,

$$V_{eff+} = V_+ - 50 \text{ volts} \tag{7}$$

based on the experimentally observed snapover in the electron collection data. The value of f in equation (6) was taken as 0.05 (i.e. 5% exposed metal) for both voltage polarities ($V_+ < 200$ V), and for both sides of the array.

Equation (1) becomes

$$2\, j_{eo}\ell_+\left[w + \pi\left(\frac{4\epsilon_o}{9}\sqrt{\frac{2e}{m_e}}\frac{V_{eff+}^{3/2}}{j_{eo}}\right)^{1/2}\right] = N_-\, j_{io}\left(1 + \frac{1.36\sqrt{10^{-3}V_-}}{1 + 40/10^{-3}V_-}\right)\ell_- - \left[w + \pi\left(\frac{4\epsilon_o}{9}\sqrt{\frac{2e}{m_i}}\frac{(0.05\,V_-)^{3/2}}{j_{io}}\right)^{1/2}\right] \tag{8}$$

with

$$j_{eo} = \eta_e e \sqrt{\frac{kT_e}{2\pi m_e}}$$

$$j_{io} = \left\{ \begin{array}{ll} \eta_i e \sqrt{\dfrac{kT_i}{2\pi m_i}} & \text{isotropic collection } 2 \\ \eta_i e v_{sc} & \text{ram collection } 1 \end{array} \right\} = N_-$$

$$V_{eff+} = \begin{cases} 0.05\, V_+ & V_+ \lesssim 200 \text{ volts} \\ V_+ - 50 & V_+ < 200 \text{ volts} \end{cases}$$

$$\left. \begin{array}{l} w = 20 \text{ m} \\ \dfrac{\ell_+}{\ell_-} = \dfrac{V_+}{V_-} \\ \ell_+ + \ell_- = 250 \text{ m} \\ V_+ + V_- = \dfrac{1}{2} V_{op} \end{array} \right\} \qquad (9)$$

In the definitions of j_{eo} and j_{io}, T_e and T_i are the temperatures of the electrons and ions, respectively, and v_{sc} is the velocity of the space system through the plasma.

Equation (8) can be solved subject to conditions (9) to yield V_+, V_-, ℓ_+ and ℓ_-. The electron and ion currents collected can then be determined. The parasitic current due to the plasma is at equilibrium,

$$I_{PLASMA} = j_e A_+ = j_i A_- \qquad (10)$$

This calculation was carried out for an environment characteristic of a 400 km orbit[18] (see table I). Since v_{sc} is greater than the ion thermal velocity, the calculation was done for both isotropic and ram collection conditions. Results are shown in figure 7. The line labeled I_{ARRAY} indicates the current which is developed by a 500 kw array at operating voltage V_{op}. The parasitic current I_{PLASMA} represents a loss of current (and therefore power) available to the load. The curves indicate that about a 10% loss of current is expected for an operating voltage of 10 kV in the ram collection configuration, and a total loss of current by $V_{op} = 60$ kV. For the isotropic collection condition, 10% loss occurs around $V_{op} = 45$ kV. A sun-oriented array will cycle between the isotropic and ram conditions twice per orbit (ignoring eclipse for the moment).

The apparent negative voltage shifts about 10% through the cycle, while the parasitic current shifts about an order of magnitude.

The bars on the current curves in figure 7 indicate the region of V_{op} where the predicted negative voltage (V_-) is in the range -750 to -1000 volts; this is the range of applied voltages which has been observed to result in arcing during laboratory experiments. According to the model, this arcing range is reached well before the parasitic current drain becomes prohibitive. This arcing phenomenon is believed to be a technology problem in array design, and not to represent any absolute limit on array operating voltage.

These results indicate that the interactions of thermal plasmas with space systems must be considered in the design of the large high voltage systems of the future. Both the parasitic currents and the arcing must be understood and techniques developed for eliminating their effects on space systems. As figure 7 indicates, it is not surprising that these effects have not presented spacecraft power system difficulties for systems flown to date. The highest operating voltage which has been used for spacecraft power systems is 100 volts, on Skylab. The model predicts parasitic currents of 0.03% (ram) and 0.003% (isotropic) for a 100 volt system. Losses of this magnitude are negligible.

The calculation of floating voltages and parasitic currents was also done for the quiescent geosynchronous environment (i.e. no substorm activity). The environment parameters[14] used are given in table II. Results of the calculation are shown in figure 8, with the results of the 400 km calculation drawn in for comparison. There is no ram effect in this case, since the ion thermal velocity is greater than the spacecraft orbital velocity. The parasitic current at geosynchronous is small (<5% of array current) for all operating voltages considered. There is the possibility of arcing for operating voltages >16 kV, based on the experimentally observed breakdowns at negative voltages of 8-10 kV for simulated geosynchronous conditions.

There are several assumptions in the model used here which are worthy of note. First, it has been assumed that the array operating voltage is unaffected by any parasitic currents collected. In the real situation, the parasitic currents will shift the operating points of the solar cells, and cause the array voltage to fall until some equilibrium is reached. The amount of shift in operating voltage of a given string of solar cells will depend on its "position" in the array ("position" here refers to both physical location and electrical configuration) and the voltage-current characteristics of the cells. Because this loading effect has

not been included in the present calculations, the results should not be taken as a quantitative description of the parasitic currents collected; they merely give an indication of the range of design operating voltages which can be expected to be severely impacted by this class of interactions.

Secondly, the modeling has assumed planar sheath growth (by using the Child-Langmuir formula for r_s) throughout. This assumption becomes less valid as plasma density decreases and as voltage increases. Thus the model predictions are more reliable for the low Earth orbit case than for geosynchronous. In particular, the predictions at large operating voltages in geosynchronous orbit should be interpreted as order of magnitude estimates.

Thirdly, no attempt has been made here to account for the effects of magnetic fields on the current collection. There are at least two sources of magnetic fields: the Earth's field and any space system fields. In general, the presence of a magnetic field is expected to reduce the current that will be collected. It may be possible to "shield" the system by an appropriate configuration driving currents to create magnetic fields. This possibility should be assessed during total system design and optimization.

Finally, effects due to photoelectron emission and/or collection have not been included in the model. Its impact on the results can, however, be estimated. The current density due to photoemission should be of order 10^{-5} amps/m^2. This is small compared to electron and ram ion current densities at 400 km, and about equal to the random ion current. The maximum total photocurrent available for collection can be estimated as $(\ell \times w)\times 10^{-5} = 0.05$ amp. Since this is small compared to the plasma currents (except for the low voltage isotropic case) at 400 km, the calculation should not be affected greatly. In the case for the geosynchronous environment, the photocurrent density is greater than the thermal current density for both electrons and ions. It is therefore possible that the photocurrent will dominate the equilibration, i.e. that the positive and negative voltages at equilibrium will be approximately equal. Since the total photocurrent is a 0.05 amp, the current collected may increase to that level; however, it still does not provide enough parasitic current to impact array operation seriously. The effect of shifting the relative magnitudes of the positive and negative voltages so that they were approximately equal would be to shift the "expected onset of arcing" point towards higher operating voltages.

The conclusion reached is, then, that the interactions of high voltage systems with the thermal plasma environment must be considered in the design of high

voltage systems for space applications. The possible detrimental effects to be avoided are excessive parasitic currents and arcing. While the calculations here have all been related to a hypothetical solar array, any high voltage component exposed to the environment can be expected to interact in the same general fashion.

SUMMARY AND CONCLUSIONS

Interactions of high voltage systems with the thermal plasma environment can give rise to parasitic current collection by high voltage systems (effectively a power loss mechanism) and to arcing for portions of the system sufficiently negative with respect to plasma potential. The simple analysis presented here indicates that the parasitic currents are of significant concern for systems with operating voltages of ~10 KV or greater in low Earth orbit. Parasitic currents are not expected to be of great concern for systems at geosynchronous (at least for operating voltages <100 KV, the highest considered here). The arcing of negatively biased segments of the system appears to be a potential problem for floating systems with operating voltages $\gtrsim$1.5 KV in low Earth orbit and with voltages >16 KV in geosynchronous. Design guidelines for high voltage systems are thus required. A program to investigate these phenomena and to develop the required design criteria is now underway at the Lewis Research Center.

The interactions discussed here are not believed to present insurmountable obstacles to future space systems. It is necessary however to design the new systems for space applications with an understanding of the ways in which their environments can affect them in mind.

REFERENCES

1. Outlook for Space. NASA SP 386, 1976.
2. Johnson, R. D.; and Holbrow, C.: Space Settlements, A Design Study. NASA SP 413, 1977.
3. Woodcock, G. R.: Solar Satellites, Space Key to our Power Future. Astronaut. Aeronaut., vol. 15, no. 7/8, July/Aug. 1977, p. 30.
4. Satellite Power System (SPS) Feasibility Study, Rockwell International, SD 76-SA-0239-1 and SD 76-SA-0239-2, Contract NAS8-32161, 1976.
5. Oman, H.; and Springate, W. F.: High Voltage Solar Array Study. (D2-121734-1, Boeing Co., Seattle; NASA Contract NAS3-11534.) NASA CR-72674, 1969.

6. Deforest, S. E.; and McIlwain, C. E.: Plasma Clouds in the Magnetosphere. J. Geophys. Res., Vol. 76, no. 16, June 1, 1971, pp. 3587-3611.
7. DeForest, S. E.: Spacecraft Charging at Synchronous Orbit. J. Geophys. Res., vol. 77, no. 4, Feb. 1, 1972, pp. 651-659.
8. Lovell, R. R.; et. al.: Spacecraft Charging Investigation: A Joint Research and Technology Program. Spacecraft Charging by Magnetospheric Plasmas, A. Rosen, ed., AIAA Progress in Astronautics and Aeronautics Series, Vol. 47, MIT Press, 1976.
9. Grard, R. J. L., ed.: ESLAB Symposium on Photon and Particle Interactions with Surfaces in Space, 6th., Noordwijk, The Netherlands, Sept. 1972, D. Reidel, 1973.
10. Rosen, A., ed: Spacecraft Charging in Magnetospheric Plasmas. AIAA Progress in Astronautics and Aeronautics Series, Vol. 47. MIT Press, 1976.
11. Pike, C. P.; and Lovell, R. R., eds: Proceedings of the Spacecraft Charging Technology Conference. NASA TM X-73537, 1977; AFGL-TR-77-0051 (Air Force Surveys in Geophysics, No. 364.)
12. Chen, F. F.: Electric Probes. Pure and Applied Physics, Vol. 21, Plasma Diagnostic Techniques, R. H. Huddlestone and S. L. Leonard, eds., Academic Press 1965, pp. 113-119.
13. Berkopec, F. D., Stevens, N. J., and Sturman, J. C.: The Lewis Research Center Geomagnetic Substorm Simulation Facility. NASA TM X-73602, 1976.
14. Kennerud, K. L.: High Voltage Solar Array Experiments. (Boeing Aerospace Co., Seattle; NASA Contract NAS3-14364.) NASA CR 121280, 1974.
15. Bayless, J. R.; Herron, B. G.; and Worden, J. D.: High Voltage Solar Array Technology. AIAA Paper 72-443, Apr. 1972.
16. Katz, I., et. al.: Three Dimensional Dynamic Study of Electrostatic Charging in Materials. (SSS-R-77-3367, Systems Science and Software, La Jolla, Cal.; NASA Contract NAS3-20119.) NASA CR 135256, 1977.
17. Parks, D. E., and Katz, I.: Solar Electric Propulsion Thruster Interactions with Solar Arrays. (SSS-R-78-3420, Systems Science and Software, La Jolla, Cal.; NASA Contract NAS3-20119.) NASA CR 135257, 1977.
18. Liehmon, H. B.: Electrical Charging of Shuttle Orbiter. IEEE Trans. Plasma Sci., vol. PS-4, no. 4, Dec. 1976, pp. 229-240.

Table 1

400 KM ENVIRONMENT

ions: 0^{+}_{16}: $\eta_o = 2\text{x}10^{11}/\text{m}^3$

$kT_i = 0.09$ eV

$$\frac{kT_i}{2\pi m_i} = 0.29 \text{ km/sec}$$

electrons: e^-: $\eta_o = 2\text{x}10^{4}/\text{m}^3$

$kT_e = 0.22$ eV

Spacecraft orbital velocity: 7.7 km/sec

Current densities:

$j_{io} = 9.4\text{x}10^{-6}$ amp/m^2 (isotropic)

$j_{io} = 2.6\text{x}10^{-4}$ amp/m^2 (ram)

$j_{eo} = 2.4\text{x}10^{-3}$ amp/m^2 (isotropic)

Table 2

GEOSYNCHRONOUS THERMAL ENVIRONMENT

ions: H^+: $\eta_o = 9.0\text{x}10^{7}/\text{m}^3$

$kT_i = 1.35$ eV

$$\frac{kT_i}{2\pi m_i} = 4.53 \text{ km/sec}$$

electrons e^-: $\eta_o = 9.5\text{x}10^{7}/\text{m}^3$

$kT_e = 1.35$ eV

Spacecraft orbital velocity: 3 km/sec

Current densities:

$j_{io} = 7\text{x}10^{-8}$ amp/m^2 (isotropic)

$j_{eo} = 3\text{x}10^{-6}$ amp/m^2 (isotropic)

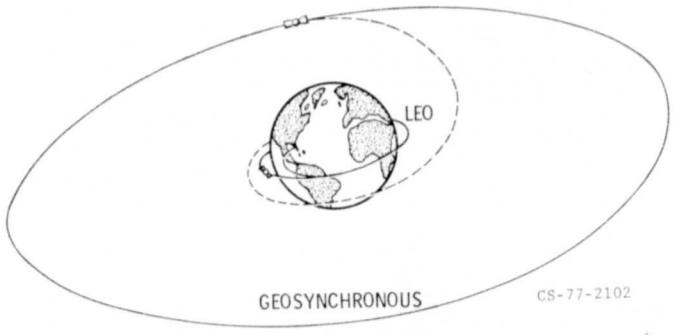

Figure 1. - Earth orbits considered.

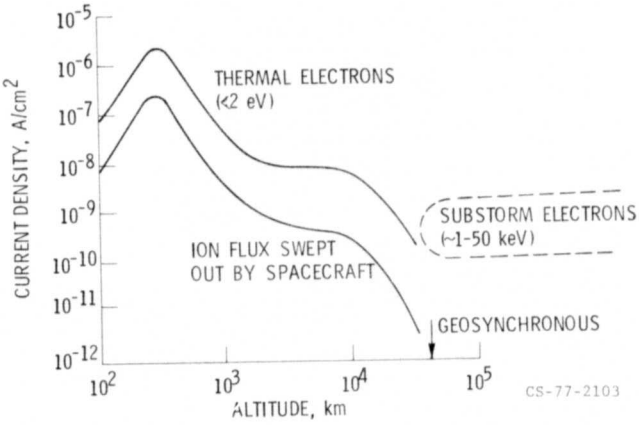

Figure 2. - Orbital charged particle environments.

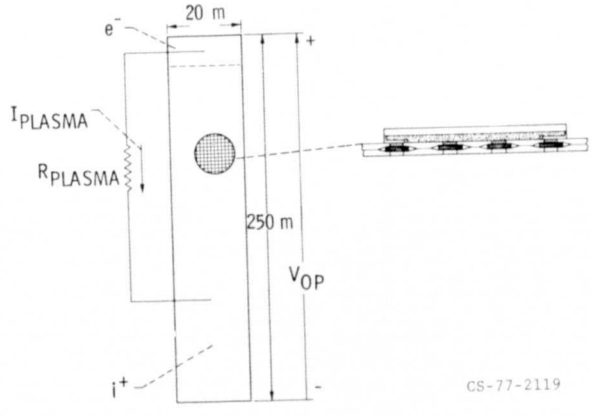

Figure 3. - Large solar array interaction model 500 kW array.

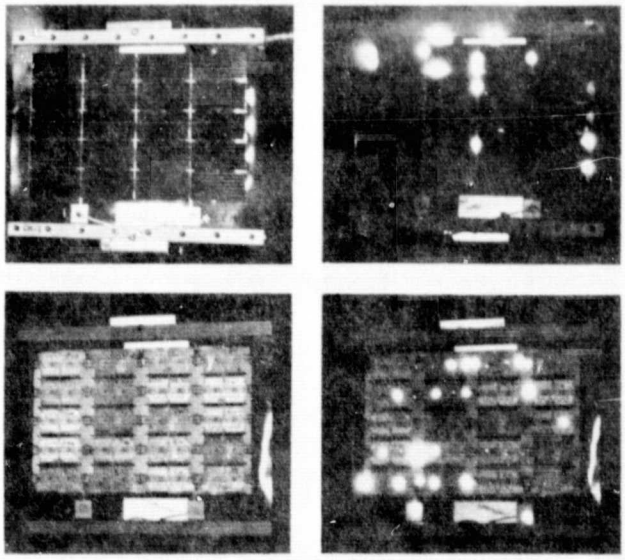

ARCING ON SOLAR CELL ARRAY SAMPLES
2x4 cm WRAPAROUND CELLS ON KAPTON
-1 kV BIASED ARRAY CIRCUIT
10^5 cm^{-3} N PLASMA

NASA/LEWIS RESEARCH CENTER
CS-77-2144 ENVIRONMENTAL INTERACTIONS PROGRAM

Figure 4. - Pictures of array (composite).

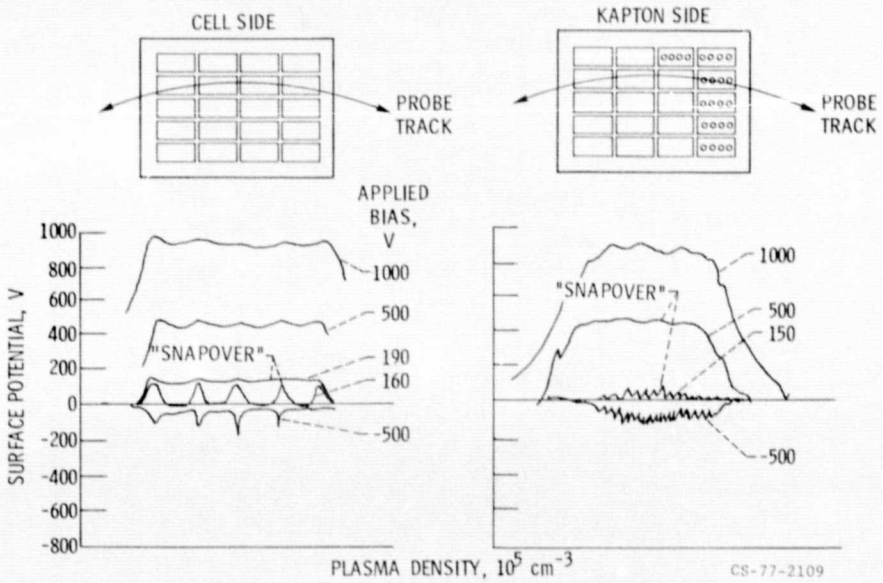

Figure 5. - Experimental results.

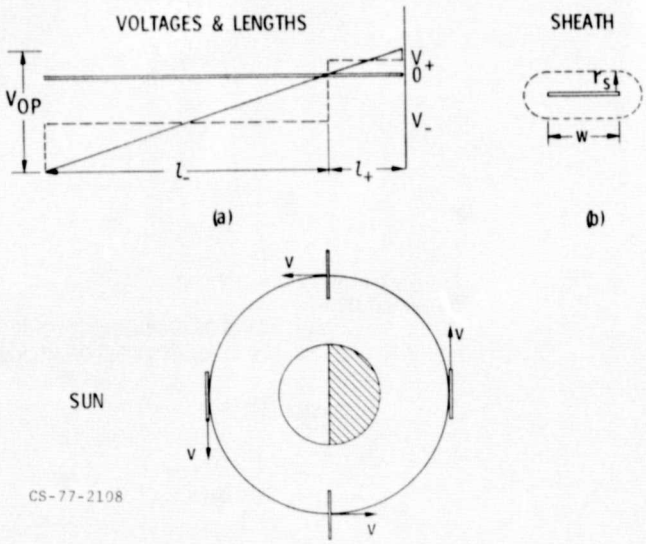

(c) LOW EARTH ORBIT SOLAR ARRAY.

Figure 6. - Interaction computation models.

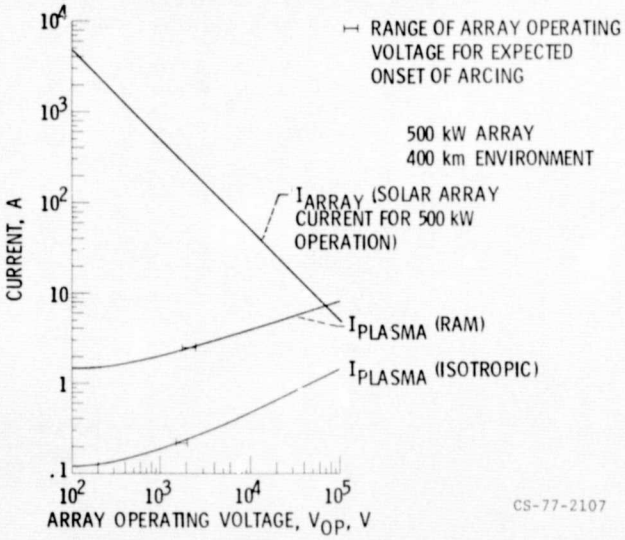

Figure 7. - Plasma/solar array coupling currents vs solar array operating voltage for a 500 kW array; in thermal environments: 400 km environment.

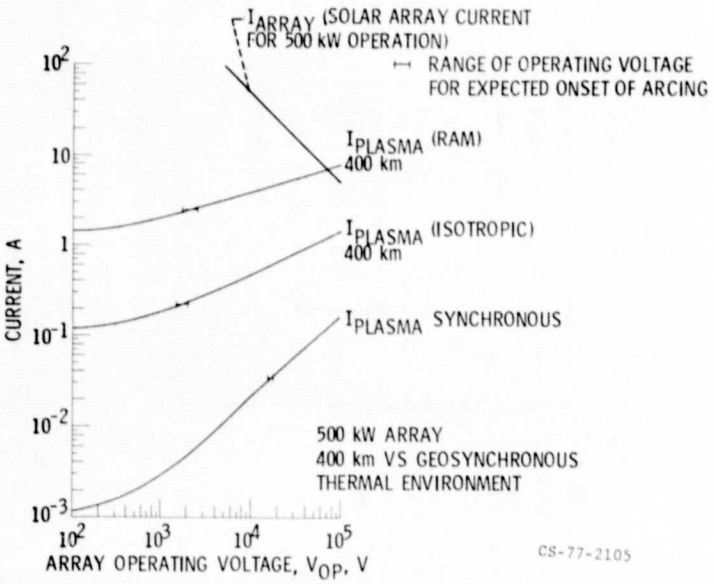

Figure 8. - Plasma/solar array coupling currents vs solar array operating voltage for a 500 kW array; in thermal environments; 400 km vs geosynchronous.